Published in final edited form as:
Hum Brain Mapp. 2011 May ; 32(5): 784–799. doi:10.1002/hbm.21066.

Sub-Patterns of Language Network Reorganization in Pediatric Localization Related Epilepsy: A Multisite Study

Xiaozhen You[1], **Malek Adjouadi**[1,*], **Magno R. Guillen**[1], **Melvin Ayala**[1], **Armando Barreto**[1], **Naphtali Rishe**[1], **Joseph Sullivan**[2], **Dennis Dlugos**[2], **John VanMeter**[3], **Drew Morris**[4], **Elizabeth Donner**[4], **Bruce Bjornson**[5], **Mary Lou Smith**[4,6], **Byron Bernal**[7], **Madison Berl**[8], and **William D. Gaillard**[3,8,9]

[1]College of Engineering and Computing, Florida International University, Miami, Florida [2]Children's Hospital of Philadelphia, Philadelphia, Pennsylvania [3]Department of Neurology, Georgetown University, Washington, District of Columbia [4]Hospital for Sick Children, Toronto, Ontario, Canada [5]BC Children's Hospital, Vancouver, British Columbia, Canada [6]Department of Psychology, University of Toronto, Toronto, Ontario, Canada [7]Miami Children's Hospital, Miami, Florida [8]Department of Neurosciences, Children's National Medical Center, George Washington University, Washington, District of Columbia [9]Clinical Epilepsy Section, NINDS, NIH, Bethesda, Maryland

Abstract

To study the neural networks reorganization in pediatric epilepsy, a consortium of imaging centers was established to collect functional imaging data. Common paradigms and similar acquisition parameters were used. We studied 122 children (64 control and 58 LRE patients) across five sites using EPI BOLD fMRI and an auditory description decision task. After normalization to the MNI atlas, activation maps generated by FSL were separated into three sub-groups using a distance method in the principal component analysis (PCA)-based decisional space. Three activation patterns were identified: (1) the typical distributed network expected for task in left inferior frontal gyrus (Broca's) and along left superior temporal gyrus (Wernicke's) (60 controls, 35 patients); (2) a variant left dominant pattern with greater activation in IFG, mesial left frontal lobe, and right cerebellum (three controls, 15 patients); and (3) activation in the right counterparts of the first pattern in Broca's area (one control, eight patients). Patients were over represented in Groups 2 and 3 ($P < 0.0004$). There were no scanner ($P = 0.4$) or site effects ($P = 0.6$). Our data-driven method for fMRI activation pattern separation is independent of a priori notions and bias inherent in region of interest and visual analyses. In addition to the anticipated atypical right dominant activation pattern, a sub-pattern was identified that involved intensity and extent differences of activation within the distributed left hemisphere language processing network. These findings suggest a different, perhaps less efficient, cognitive strategy for LRE group to perform the task.

Keywords

brain activation pattern; data-driven clustering; fMRI; epilepsy; language; PCA-based decisional space

[*]Correspondence to: Malek Adjouadi, College of Engineering and Computing, Florida International University, 10555 W. Flagler Street, EC 2672, Miami, FL 33174. adjouadi@fiu.edu.

INTRODUCTION

Epilepsy populations provide an important window into capacity for neural plasticity as the location of essential brain functions needs to be identified for epilepsy surgery. It is known from long experience that several essential domains are perturbed by epilepsy or its underlying causes. Although there are studies that have examined motor control [Muller et al., 1998a], declarative memory, and working memory networks [Dupont et al., 2000; Powell et al., 2008; Rabin et al., 2004; Richardson et al., 2004], most interest has focused on language systems. Notably, there is a higher incidence of atypical language dominance in epilepsy populations [Gaillard et al., 2007; Rasmussen and Milner, 1977; Springer et al., 1999; Thivard et al., 2005; Woermann et al., 2003]. The functional anatomy of language processing networks has been extensively studied through intracarotid amobarbital test (IAT) [Rasmussen and Milner, 1977], ^{15}O-water-PET [Blank et al., 2002; Muller et al., 1998b; Petersen et al., 1988; Wise et al., 1991], and fMRI [Binder et al., 1995; Bookheimer, 2002; Cabeza and Nyberg, 2000; Just et al., 1996]. Language is typically left hemisphere dominant, but there are recognized variants (bilateral or right dominance) in normal right-handed (prevalence≈5%) and left-handed populations (≈22%) [Pujol et al., 1999; Rasmussen and Milner, 1977; Springer et al., 1999; Szaflarski et al., 2002; Woods et al., 1988]. Furthermore, patients with localization related epilepsy (LRE) exhibit a higher prevalence of atypical language dominance (20–30%). Most fMRI studies are based on visual [Fernandez et al., 2001; Gaillard et al., 2002, 2004] or ROI asymmetry indices [Binder et al., 1996; Frost et al., 1999; Gaillard et al., 2002, 2007; Ramsey et al., 2001; Spreer et al., 2002; Woermann et al., 2003] and only examine inter-hemispheric “re-organization.” Other studies examine regional differences but also rely either on ROI asymmetry indices or regression analysis on clinical variables [Berl et al., 2006; Billingsley et al., 2001; Gaillard et al., 2007; Voets et al., 2006; Weber et al., 2006] all depending on presumptions of where language “activation” is “known” to occur based on understanding of normative data. There are ECS studies that purport to examine intra-hemispheric differences [Hamberger et al., 2007; Ojemann et al., 2008], but these do not have control data and can not examine language processing outside the surgical field.

Atypical language patterns may represent: (1) “re-organization,” where the primary region of language processing has moved or (2) “compensation,” where additional areas are recruited within the broadly distributed networks that support language and ancillary cognitive domains to assist in language processing. Most commonly, studies have identified inter-hemispheric shifts to the right homologues of Broca’s and Wernicke’s areas that are generally understood to reflect “re-organization” [Gaillard et al., 2002, 2004, 2007; Staudt et al., 2001, 2002]. Intra-hemisphere “reorganization” or “compensation” studies are less common. Using comparison of activation maxima, there is modest evidence for greater variance in temporal regions and a shift in temporal activation posteriorly and superiorly in left hemisphere seizure focus patients who remain left dominant [Rosenberger et al., 2009]. Using a principal component analysis (PCA) of difference maps between a group of normal left hemisphere dominant controls and individual patients with LRE, a subgroup of patients with recruitment of posterior temporal areas was also found; atypical language appeared restricted to the distributed language network homologues and margins [Mbwana et al., 2009]. It may be difficult to know from these studies whether modest shifts in activation point maxima or recruitment of brain areas on the margins of established networks represent “compensation” or “re-organization.” However, one form of “compensation,” based on intensity level differences instead of location, may not be identified by current methods. This is because intensity normalization is traditionally used as a pre-processing step to scale a group of fMRI activation maps to the same intensity range. For example, sub-profile modeling (SSM) uses the natural-log transformation as the first step to standardize the raw image matrix [Alexander and Moeller, 1994].

One of the limitations of functional imaging studies is the assumptions that study populations are homogeneous and that a given paradigm will recognize a single unvarying network identified by the experimental task. Clinical practice with patient populations, particularly involving language, suggests those assumptions are false. Patient populations of developmental and other disorders are also flawed by their assumption that patient populations are distinct form control populations in a uniform way. Some recent studies of executive functions in attention deficit hyperactivity disorder (ADHD) populations used regression analysis to help characterize patient and control populations. They show there is a spectrum within the patient population. Some ADHD children, who do better on given measures, may more closely resemble controls [Vaidya, 2005]. However, these studies are only able to interrogate their data where they find activation derived from limited datasets. Normal or pathological variants are lost in such approaches [Berl, 2006]. To overcome such limitations, it is necessary to examine large populations with controls and patients by a data driven means to identify variant sub patterns. This approach does not assume controls and patients are different, rather it allows that both patients and controls may be distributed across subgroups and allows for the ability to analyze subgroups based on clinical or other experimental features.

Limitations of standard approaches motivate the need to design objective methods for identifying language activation patterns. Previous methods are often constrained in their analyses either for the straightforward left–right differences, subjectivity associated with the use of visual rating and/or selection of ROI, or the use of data that lacks heterogeneity. In general, most group analyses of fMRI datasets look for “commonality” under the assumption of the homogeneity of the sample [Berl et al., 2005; Price et al., 2006]. Moreover, other PCA studies have not included a large group of normal controls who may have atypical language representation [Mbwana et al., 2009].

We aimed to develop a PCA-based method to identify common and variant language activation patterns (shared) among control and epilepsy groups independent of a priori assumptions and biases inherent to region of interest and visual analyses [Gaillard, 2004; Liegeois et al., 2004; Szaflarski et al., 2006]. PCA provides an unbiased data-driven group separation within any given population by selecting the informative primary cluster members. Furthermore, we did not perform inter-subject intensity normalization of the previously normalized intra-subject data, thus avoiding the loss of a potentially important source of variance. Segmentation methods, such as support vector machine and discriminant analysis, are classifier methods based on supervised training, where previous knowledge of the datasets is implicit. The proposed method takes a different approach in the clustering process on the basis of the PCA eigenspace. We are neither trying to categorize each subject into simple left–right dominance to replace the conventional clinical methods, nor striving to separate normal subjects from patients. On the basis of the distinct activation patterns identified by our data-driven method, we then sought to gain insights into brain plasticity and compensation by examining the subjects in each language activation pattern by distinguishing features including control/patient designation, handedness, seizure focus location, and age of epilepsy onset.

Individual epilepsy centers are unlikely to evaluate a sufficient number of patients in a short time frame to identify variant activation patterns informed by heterogeneous clinical variables, collaborative efforts are needed. Therefore, we established a consortium of pediatric epilepsy centers to collect functional imaging data using common paradigms and similar acquisition parameters. We aimed to verify similarity of findings across sites, and establish data-driven methods to reliably identify sub-patterns of language processing from pooled data.

METHODS

Data Source

Florida International University (FIU), in collaboration with five pediatric hospitals with active epilepsy surgery programs, established a multisite consortium for control and pediatric epilepsy data collection (http://mri-cate.-fiu.edu) to facilitate fMRI group studies in LRE patients [Lahlou et al., 2006]. The fMRI data and relevant clinical measures were stored in the data repository for central standardized processing.

There were 133 fMRI datasets with their corresponding anatomical T_1 MRIs that were obtained using the data repository mri-cate.fiu.edu. There were 11 datasets with null activation, even under modified $P = 0.1$ uncorrected condition, which were excluded in the analysis. Valid datasets from 64 control and 58 children with LRE (patient population) were thus included in this study as shown in Table I. The basic demographic data is included in Table II. Procedures were followed in accordance with local institutional review board requirements; all parents gave written informed consent and children gave assent. Typically developing control subjects were required to be right handed (the Harris tests of lateral dominance) and free of any current or past neurological or psychiatric disease. The mean age of patients was 13.86 years (range: 4.5–19 years), with mean age seizure onset 8.23 years (range: 1–18 years). There are 26 left localized patients, from which 17 (65%) had temporal focus and the rest with extra-temporal focus. There are 18 right localized patients, from which seven (39%) had temporal focus and the rest had an extra-temporal focus. Three patients had bilateral seizure focus. Twenty-two patients had abnormal MRI: seven tumor; five mesial temporal sclerosis; four focal cortical dysplasia; one vascular malfunction; three focal gliosis; and two atrophy. Of the 45 patients with seizure etiology information, 21 had remote symptomatic seizure etiology, 21 cryptogenic, and three acute symptomatic. Eleven patients (out of the 54 available) had atypical handedness (left or ambidextrous) as determined by clinical assessment or handedness inventories such as the Harris tests of lateral dominance or the modified Edinburgh inventory [Harris, 1974; Oldfield, 1971].

Image Acquisition and Paradigm

For all the participating institutions, each subject was asked to perform an auditory description decision task (a word definition task) which was designed to activate both temporal (Wernicke's area) and inferior frontal (Broca's area) cortex [Gaillard et al., 2007]. The task required comprehension of a phrase, semantic recall, and a semantic decision. Each institution had unique acquisition parameters that were subsequently corrected and standardized. The block design paradigm consisted of 100 (TR = 3 s) or 150 (TR = 2 s) time-points, with experimental and baseline periods alternating every 30 s for five cycles, totaling 5 min. During the "on" period, the participant listened to a definition of an object followed by a noun. Participants were instructed to press a button each time they judged that the description matched the noun. For instance, "a long yellow fruit is a banana" (true response) or "something you sit on is spaghetti" (Not true). Definitions occurred every 3 s. Matching pairs were pseudo-randomly distributed (70% true responses and 30% foils). During baseline, the subject listened to the task definitions presented in reverse speech. The participant was instructed to press a button each time he/she heard a tone that followed the auditory string (70% true responses and 30% foils). The baseline was designed to control for first and second order auditory processing, attention, and motor response, while engaging the broad language processing network on an individual basis necessary for effective pre-surgical evaluation [Gaillard et al., 2007; Mbwana et al., 2009]. Four age appropriate levels of difficulty were available (4–6, 7–9, 10–12, >12). The difficulty level was achieved by manipulating the task vocabulary based on word frequency normative data derived from reading materials [Carroll et al., 1971].

Data Preprocessing

The participating institutions provided the anatomical and fMRI datasets using distinct file formats, plane of exam, view orientation, slicing, voxel size, TR, and number of time points. In addition, data were obtained from either 1.5 or 3.0 T magnets. Orientation and field of view were corrected and standardized. Datasets were matched into Neuroimaging Informatics Technology Initiative (NIFTI) format using the transversal view and radiology convention, and were finally mapped into the standard Montreal Neurological Institute (MNI) brain with $3 \times 3 \times 3$ (mm^3) voxel size and resolution of $61 \times 73 \times 61$ (axial × coronal × sagittal).

A set of scripts in MATLAB (The MathWorks) was developed to perform the needed correction and standardization for group analysis. The fMRIB Software Library (FSL) was used to perform the pre- and post-processing required for obtaining the resulting 3D activation maps [Jenkinson et al., 2002; Jenkinson and Smith, 2001; Rowe and Hoffmann, 2006; Woolrich et al., 2001]. The data preprocessing was performed using MCFLIRT [Jenkinson et al., 2002]; brain extraction using BET [Smith, 2002]; spatial smoothing using Gaussian kernel of FWHM 8 mm; intra-subject mean-based intensity normalization of all volumes by the same factor; high pass temporal filtering [Gaussian-weighted least square fitting (LSF) straight line fitting, with sigma = 120.0 s]. Time-series statistical analysis was carried out using FMRIB's improved linear model (FILM) with local autocorrelation correction [Woolrich et al., 2001]. Post-processing was performed using fMRI Expert Analysis tool (FEAT) generating Z (Gaussianized T/F) statistic images thresholded using clusters determined by $Z > 2.3$ and a (corrected) cluster significance threshold of $P = 0.05$ [Forman et al., 1995; Friston et al., 1994; Worsley et al., 1992]. Registration to high-resolution and standard images was carried out using FLIRT [Jenkinson et al., 2002].

PCA-Based Decisional Space Separation

According to the concept and merit of subject loading, we performed the PCA on the 122 fMRI activation maps without masking or applying Z value normalization across subjects, by arranging 3D data into a 2D matrix where each subject's data constitutes a specific column. An eigen-system was then generated. On the basis of the relationship among the top eigenvectors, general lateralization, and intensity difference, as well as the dendrogram of the Euclidian distance matrix of the PCA, criteria were decided for the top two eigenvectors of the PCA-based decisional space which identified three primary clusters (the first as major group left dominant, the second featured higher intensity levels, and the third with right dominant activation). The 75 undecided cases were then projected onto a new decisional space based on the PCA of only those datasets that initially were identified as belonging to the three primary clusters. By using the modified-Euclidean distance method, the 75 undecided cases were then classified in the new decisional space into one of the three primary clusters initially determined, using unique mathematically derived thresholds [You et al., 2009]. The detailed implementation steps and the mathematical foundation of this method that drive the clustering decisions are provided in Appendices A and B.

Fisher exact test was applied to assess the site independence as well as the significance of association for signal intensity grouping versus either magnet strength or control/patient grouping. The association of clinical factors with the group distribution was analyzed using either Fisher exact test for categorical data or ANOVA and t-test for continuous data. If the overall Fisher exact test was significant, pairwise comparisons of groups were performed. The Holm's sequential Bonferroni procedure was then applied to correct for the probability of a Type I error ($\alpha = 0.05$).

Group Map and Significance Map

To verify and understand the separation results of PCA, the range and location of group member variability were assessed with the mean group map. A significance map for each group was generated. This map is different than the collective penetrance maps used by others [Mbwana et al., 2009; Seghier et al., 2008], as we sought the commonality contribution of each subject to the mean map. On the basis of the histogram of each mean group map, a mask containing 90% of the activation energy was defined. The group significance map is then computed by first masking each individual activation map (within each group), then calculating the commonality significance value as defined in Eq. (1).

$$C_S = e^{-\frac{(\text{Value}_{\text{Voxel}} - \text{Mean})^2}{2\text{SD}^2}} \quad (1)$$

The commonality significance (C_S) value is calculated for each voxel within the masked area, and then the total group significance map is generated by averaging the C_S values across the subjects within a given group. This provides a visual representation of the areas that have a significant percentage of subjects sharing the same location of activation.

RESULTS

Activation Patterns and Significance Maps

The PCA analysis identified three distinct groups of subjects after the self-separation process using the top subject loadings and distance method. The activated areas of the three group activation patterns broadly encompass Broca's and Wernicke's areas. Group 1 exhibited activation in the left hemisphere (Fig. 1a and Table III). Group 2 (Fig. 1b) consisted of a cluster of subjects that shared the same general activation areas as Group 1; however, the magnitude of activation for Group 2 was stronger than those of Group 1, especially in Broca's area, as shown in Fig. 1b and Table III, and additional activation was evident in left MFG (BA 46, 9), left SMA (BA 6), and right cerebellum. Group 3 had activation in right hemisphere homologues (Fig. 1c and Table III). The distribution of patients and controls differed among the three groups ($P < 0.0004$). Group 1 consisted of nearly all the healthy controls and a majority of patients; Groups 2 and 3 were composed principally of patients but included a few typically developing controls. In terms of typical language activation, LRE patients had greater magnitude of activation than controls based on the subjects distribution in Groups 1 and 2 (Fisher Exact Test; $P = 0.0005$).

To appraise the subjects' contribution for each group map, a group significance map was generated for each group as shown in Figure 2. This figure helps to visualize the variance of the separation results comparing the group members with the group map. The maximum commonality significance value for the three groups are higher than 0.8; Group 1 has the least variance and Group 3 has the most variance.

Table III provides the mean map's activation maxima of each small cluster within each group and their coordinates, cluster size, the peak value of each cluster, and corresponding commonality significance value, and corresponding Brodmann Area.

A second level *t*-test was performed comparing the mean map of Group 1 to Group 2; Figure 3 depicts the areas that remain significantly different.

Sites and Scanner Effects

We contrasted Groups 1 and 2 with Group 3 on the basis of magnetic strength, since Groups 1 and 2 both exhibit typical language dominance according to PCA. We found no difference

in the effect of scanner magnetic strength in group separation of laterality category (Group 1 + 2 to Group 3) on patients (Fisher Exact Test, $P = 0.7$). We did find a magnet strength versus Groups 1–2 correlation when considering both control and patients (Fisher Exact Test, $P = 0.0005$). As no control subjects were scanned by 1.5 T, the Groups 1–2 difference may reflect control and patient groups. Magnet strength did not have an effect between Groups 1 and 2 when only patients were considered (Fisher Exact Test, $P = 0.2$). We contrasted Groups 1 and 2 with Group 3 on the basis of sites. Groups 1 and 2 were concatenated because the control subjects were scanned at only one site. We found no difference between the effect of sites in group separation (Fisher Exact Test, $P = 0.6$).

Demographic and Clinical Variables

We found no difference in age at seizure onset, duration of epilepsy, and gender between the three groups. However, there was an age difference among the three groups [ANOVA, $F(2, n = 118) = 9.44$, $P = 0.0002$]; differences were found between Groups 1 and 2 ($F = 3.78$, $P = 0.001$, Bonferroni), as well as between Groups 1 and 3 ($F = 3.16$, $P = 0.05$, Bonferroni). Group 1 was younger than Group 2 [$t(108, n = 110) = -3.91$, $P = 0.002$].

Table IV and Figure 4 present the patient's group profiles with related categorical variables and illustrate the clinical factors distribution among these three groups. There were no differences based on gender seizure focus and etiology among the three groups. Data from Groups 1 and 2 were compared first, since both groups were left lateralized but exhibited different intensities. The distribution of seizure focus between Groups 1 and 2 are different [χ^2 (13, $n = 50$) = 21.731, $P = 0.03$]; the patients of Group 2 had a higher percentage (50–34%) in terms of right seizure focus. In contrast, Group 3 with right activation was largely male (6 out of 8), left handed (5 out of 8), with a left seizure focus (6 out of 8), and had a history of (poorly controlled) symptomatic LRE (**6**). Patients' data were then compared between Group 1 and Group 3. Patients in Group 3 had a higher percentage of left seizure focus than in Group 1 (71.4% vs. 53%); the handedness distribution is also different from Group 1 (Fisher Exact Test, $P = 0.007$; Table V). The other clinical variables—age, gender, age of onset, and seizure duration—were not different between these two groups. Data were then compared between the two broad groups, left lateralized (Group 1 + 2) and right lateralized (Group 3); the handedness difference was significant (Fisher Exact Test, $P = 0.003$) and left-handed patients tended to have right hemisphere activation (Group 3, Fisher Exact Test, $P = 0.002$; Table V). No significant difference of seizure etiology or seizure focus was found between these two broad groups.

DISCUSSION

We used a new method of PCA-based decisional space to identify sub-patterns of distinct language activation patterns in control and LRE patients from different sites, who performed the same fMRI auditory description decision task. Three sub-groups were identified: two with predominantly left hemispheric activation but with different regional weighting of activity, and one with a predominantly right-sided activation pattern. Normal controls as well as patients fell into each of the three groups. However, their distribution was different among the subgroups. There was a greater proportion of controls in the first group, while patients constituted the majority in the other two groups. Unlike ROI analysis used to generate an asymmetry index, our method did not provide determination of language dominance, but aimed to identify distinct activation patterns. These findings provide insight into reorganization of language system functions and potential compensatory strategies in epilepsy and normal populations.

Different PCA-based methods have been used to identify fMRI activation patterns [Andersen et al., 1999; Viviani et al., 2005] but only at an intra-subject level. fMRI

activation analysis at the inter-subject level has been used by Werder et al., [2006] in a study of a few subjects aimed at separating epilepsy patients from control subjects. Seghier et al. [2007, 2008] also used an inter-subject approach by applying a Fuzzy clustering algorithm to detect subject-specific activations to an fMRI lexical reading test in 38 normal subjects; using different variance analysis, they found sub-patterns of activations that were related to different skill sets or cognitive strategies. Mbwana et al. [2009] identified four patterns of activation among 45 patients with left hemisphere seizure foci based on PCA clustering following difference maps to see how individuals deviated on a voxel-wise basis from a normal control group. They found evidence for intra-hemispheric compensation and inter-hemispheric reorganization in three patient subgroups. However, their results were obtained after necessarily excluding the controls with atypical activation; only heterogeneity of the patient population was considered. Ford et al. [2003] also attempted to classify patients' fMRI activation maps but with a different method and in different areas, using the Fisher Linear Discriminant for Alzheimer's disease, schizophrenia, and mild traumatic brain injury. Suma et al. [2007] have also demonstrated that PCA can be used for the classification of fMRI activation maps. In their study, PCA was not directly applied to activation maps; rather PCA was applied to area and centroid values obtained from post-processing of the activation maps.

The merit of PCA eigenvectors has been explored in few fMRI studies, both in a confirmatory and a classifier manner, which are different from our study. Sugiura et al. successfully used the loadings of PCA for separating fMRI activation regions into three groups from 19 normal subjects on memory-guided saccade tasks. Their analysis was based on the assumption of the homogeneity of the normal population and required a priori knowledge of predefined region of interests as well as each region's relationship to the three main lobes. In another study, PCA with reference (PCA-R) combined with coefficient-constrained independent component analysis (CC-ICA) were used as classifiers to distinguish 28 schizophrenia patients from 25 healthy controls based on results of sensorimotor tasks [Sui et al., 2009]. This study presumed common differences between patient and control populations.

Though the PCA we used is a standard feature extraction approach, our implementation differs from other methods in several ways. For each subject in our method, the entire activation map was fed into the algorithm, without intensity normalization. Potential differences in language patterns based on extent and intensity may thus be identified. Furthermore, data segmentation was performed without a priori assumptions or subject classification: we combined typically developing and patient populations to allow the algorithm to associate statistical features based on the data and, therefore, overcoming subjectivity imposed by using selected normal subject as reference. Mathematical thresholds were uniquely derived to delineate regions for three primary clusters based on the first two eigenvectors of the PCA. Moreover, the modified-Euclidean distance method was used to assign those initially unclassified subjects into one of the three primary clusters. The motivation here is to determine to which primary cluster the activation patterns of the undecided subjects most resemble. The advantage is that the final clustering results are not grouped randomly, but taking into consideration both the most significant feature difference (top eigenvectors for primary clusters) as well as the voxel-to-voxel statistical difference in 3D images. With the increasing number of fMRI datasets made available through the consortium, the PCA-based data-driven method is well positioned to reliably identify sub-patterns of language processing from the pooled data.

Our findings suggest variants of language patterns which are not revealed in previous studies (Group 2); secondary analysis suggests the variant patterns are more common to epilepsy patients than to controls. Our methods sorted subjects by imaging features independent of

whether a child had epilepsy or was a control. The broad distinction of left and right hemisphere dominant patterns identified in our study are similar to prior studies on language dominance in normal volunteers and in epilepsy populations using transcranial-Doppler, transcranial magnetic stimulation, the intra-carotid amobarbital test, and conventional fMRI analysis [Binder et al., 1996; Fernandez et al., 2001; Gaillard et al., 2002; Khedr et al., 2002; Knecht et al., 2000; Kurthen et al., 1994; Rasmussen and Milner, 1977; Risse et al., 1997; Springer et al., 1999; Woods et al., 1988; Wyllie et al., 1991]. The right language group (Group 3) contained 7% of the total population and 14% of the LRE population which is comparable to previous typically developing and epilepsy patient studies. The majority of patients in this group had left seizure focus, was left-handed, and had left structural lesions, all factors known to be associated with atypical language dominance [Gaillard et al., 2007; Springer et al., 1999; Woermann et al., 2003]. Although activation in this group occurred in the right hemisphere in areas that mirror activation seen in the left-hemisphere patterns [Gaillard et al., 2002; Mbwana et al., 2009; Rosenberger et al., 2009; Staudt et al., 2001]—this group also showed the greatest variance. Some studies suggest that atypical language dominance in patient populations is tightly constrained to right homologues [Rosenberger et al., 2009; Staudt et al., 2001] but others suggest greater variability when language has shifted to the typically nondominant hemisphere [Voets et al., 2006]. These patterns are considered to represent “reorganization” from the left to the right hemisphere in response to epilepsy or its remote cause [Gaillard et al., 2007; Mbwana et al., 2009]. Findings in this study suggest that transfer of language dominance across hemispheres may be imperfect in some patients.

Intra-hemispheric variants, however, have been harder to identify by conventional analytic approaches. We identified two groups with left hemisphere patterns of activation. The larger group (Group 1) is composed of nearly all typically developing children and the majority of patients. We also identified another group (Group 2), composed of mostly patients and a minority of typically developing controls. This group had a different left hemisphere activation pattern than the first group. Group 2 not only showed different activation intensity in the inferior frontal regions but it also involved the recruitment of adjacent MFG (BA 46, 9), SMA (BA 6), and contralateral cerebellum. The regions observed are all areas identified with the widely distributed left hemisphere language processing network but are also those thought to be engaged in verbal working memory [Baillieux et al., 2008; Stoodley and Schmahmann, 2009]. In addition, these subjects express the highest measure of commonality, that is, the least variance in the IFG (BA 44/45). This data suggests tighter homogeneity of activation in this group than in the others. There are two possible explanations for these findings. Activation in these areas may reflect greater engagement of verbal working memory systems, possibly due to effort, perceived difficulty, effect of medications, effect of epilepsy, or compensation for impaired hippocampal memory function [Berl et al., 2005; Dupont et al., 2000]. Group 2 also had a higher percentage of patients with a right seizure focus. A right seizure focus may compromise ancillary and non linguistic aspects of language processing that occurs in the right hemisphere, requiring compensation in the left hemisphere [Berl et al., 2005]. In this view, the Group 2 left activation pattern represents “compensation” rather than “reorganization” [Berl et al., 2005; Mbwana et al., 2009] and suggests a possible remote effect on of a right hemisphere focus on traditionally left-lateralized functions. These patients may draw upon the distributed language network in a different way than most controls.

Our analysis separated subgroups by distribution of activation as well as intensity of activation. The latter was an unanticipated finding but has been seen in VBM difference map approaches and is an important basis for regression analysis of fMRI cognitive studies analyzed in relation to behavioral measures including performance [Bunge et al., 2002; Mbwana et al., 2009; Turkletaub et al., 2003, 2004; Vaidya et al., 2005]. In these

circumstances, greater magnitude of activation in narrowly defined brain areas is thought to represent greater recruitment of cortical neurons for task that may represent greater ability, learned skill, or greater effort for task performance. For our population, the data provides evidence that for a subgroup there is a differential recruitment of neural networks in that region for that task.

There are some limitations to our study. The segregation process for the intermediary value may be imperfect, since the boundaries of the primary clusters were defined based on the relationship between the top eigenvectors and the hemispheric dominance as well as between the top eigenvectors and intensity. The decision in terms of number and threshold criteria for primary cluster is based on the characteristics of our analyzed population. Thus, the boundary calculated to identify primary clusters is valid only for a mixed population with high variability of activation intensity and broad distinction of left and right hemisphere dominance. This limitation was somewhat attenuated given that the dendrogram identified three major groups present in our mixed population. It is also possible that some, less common, variant sub-patterns were not identified. On the basis of a supervised process, we identified 39% of the population into primary clusters. These primary clusters were used as references for a second round classification to sort the undecided datasets and associate them to the closest cluster. These undecided subjects did include variant activation patterns, such as bilateral activation, not represented in a straight forward manner in the primary clusters but scattered in the decisional space. Moreover, it is possible that there are differences in modulation between the nodes of the larger distributed network for processing language that may be assessed by other methods such as changes in functional connectivity [Hampson et al., 2002].

Some of the differences that characterize Group 3 may represent an effect of handedness. None of our typically developing children were left handed or ambidextrous. However, previous studies involving left handed controls (and it is not clear how many had acquired sinistrality) show that 76–78% are left dominant [Pujol et al., 1999; Szaflarski et al., 2002]. Moreover, left-handed patients are over represented in epilepsy populations; 56% or more of left-handed patients may be expected to have atypical language dominance—more than left-handed controls [Gaillard et al., 2007; Rasmussen and Milner, 1977]. These data suggest that both atypical language dominance and atypical handedness are reflections of the underlying epilepsy or its remote cause.

The differences in scanner manufacturer, magnetic strength, and acquisition parameters are often perceived as limitations that hinder group analysis on the datasets collected from a variety of sites. Standard post-processing group analysis discourages the use of different scanners, different settings, and different resolutions; however, the methods used for this study provide standardization for different formats and our analysis showed that there was no scanner or site effects in our clustering results. These findings support collaborative efforts to investigate patient populations that require substantial number of subjects to gain more insights from expected heterogeneity.

A substantial study population enhances the ability to identify variant patterns of language networks by data-driven methods and gain insight into the neurobiology of complicated cognitive processes. Multisite data collection provides larger data sets, through which additional and less common activation pattern variants can be identified. Consequently, a more comprehensive understanding of language-related clinical variables, such as seizure focus and pathological substrate, can be achieved. This information is necessary to improve care and outcomes. The PCA-decisional space presented here can be helpful in sorting an individual patient into a particular language pattern subset without the bias and limitations inherent to the traditional fMRI patient care analysis. The proposed method might also be

useful for assessing large combined patient and control datasets in which visual or ROI rating may be impractical or difficult. This is especially applicable for those developmental disorders where population differences are not readily apparent and assumptions of patient population homogeneity are unrealistic. There are conceptual limitations of language network organization when activation patterns are categorized into left, bilateral, or right dominance. Future research should take advantage of the PCA-decisional space to identify additional activation sub-pattern for epilepsy related studies.

We present a PCA-based method implemented to perform data-driven segmentation on a heterogeneous population of control and LRE subjects. We identified three subgroups with different mean activation maps. Not applying intensity normalization allowed us to consider simultaneously the location, extent, and magnitude of activation intensity; this method helped identify a subgroup with a left hemisphere activation pattern distinct form one more commonly found in normal controls and in the majority of patients. We also introduced a significance map derived from the subgroup and further analyzed the segregation results by clinical variables. Our analysis supports the notion of pooled data from several institutions using the same paradigm and comparable acquisition parameters. We do not claim that our method is better than other segregation methods. Rather, we suggest that this method applied to normal control, developmental, and patient populations may identify normal and pathological activation patterns for cognitive systems. These methods together may provide insights into mechanisms for brain compensation and neural plasticity.

Acknowledgments

Contract grant sponsor: American Epilepsy Society (Impetus and Infrastructure); Contract grant number: NINDS R01 NS44280; Contract grant sponsor: Children's Research Institute Avery Award, Intellectual and Developmental Disabilities Research Center at Children's National Medical Center; Contract grant number: NIH IDDRC P30HD40677; Contract grant sponsor: General Clinic Research Center; Contract grant number: NIH GCRC M01-RR13297; Contract grant sponsor: National Science Foundation; Contract grant numbers: HRD-0833093, CNS-0426125, CNS-0520811, CNS-0540592; Contract grant sponsors: Ware Foundation and the Joint Neuro-Engineering Program with Miami Children's Hospital (Clinical support), FIU Graduate School Dissertation Year Fellowship (Financial support).

Abbreviations

BOLD	blood oxygenation level dependent
EPI	echo-planar imaging
fMRI	functional magnetic resonance imaging
FSL	fMRIB software library
IFG	inferior frontal gyrus
LRE	localization related epilepsy
MFG	medium frontal gyrus
MNI	Montreal neurological institute
PCA	principal component analysis
SMA	supplementary motor area

References

Andersen AH, Gash DM, Avison MJ. Principal component analysis of the dynamic response measured by fMRI: A generalized linear systems framework. Magn Reson Imaging. 1999; 17:795–815. [PubMed: 10402587]

Baillieux H, De Smet HJ, Paquier PF, De Deyn PP, Marien P. Cerebellar neurocognition: Insights into the bottom of the brain. Clin Neurol Neurosurg. 2008; 110:763–773. [PubMed: 18602745]

Berl MM, Balsamo LM, Xu B, Moore EN, Weinstein SL, Conry JA, Pearl PL, Sachs BC, Grandin CB, Frattali C, Ritter FJ, Sato S, Theodore WH, Gaillard WD. Seizure focus affects regional language networks assessed by fMRI. Neurology. 2005; 65:1604–1611. [PubMed: 16301489]

Berl MM, Vaidya CJ, Gaillard WD. Functional imaging of developmental and adaptive changes in neurocognition. Neuroimage. 2006; 30:679–691. [PubMed: 16332444]

Billingsley R, McAndrews M, Crawley A, Mikulis D. Functional MRI of phonological and semantic processing in temporal lobe epilepsy. Brain. 2001; 124:1218. [PubMed: 11353737]

Binder JR, Rao SM, Hammeke TA, Frost JA, Bandettini PA, Jesmanowicz A, Hyde JS. Lateralized human brain language systems demonstrated by task subtraction functional magnetic resonance imaging. Arch Neurol. 1995; 52:593–601. [PubMed: 7763208]

Binder JR, Swanson SJ, Hammeke TA, Morris GL, Mueller WM, Fischer M, Benbadis S, Frost JA, Rao SM, Haughton VM. Determination of language dominance using functional MRI: A comparison with the Wada test. Neurology. 1996; 46:978–984. [PubMed: 8780076]

Blank SC, Scott SK, Murphy K, Warburton E, Wise RJ. Speech production: Wernicke, Broca and beyond. Brain. 2002; 125 (Part 8):1829–1838. [PubMed: 12135973]

Bookheimer S. Functional MRI of language: New approaches to understanding the cortical organization of semantic processing. Annu Rev Neurosci. 2002; 25:151–188. [PubMed: 12052907]

Bunge SA, Dudukovic NM, Thomason ME, Vaidya CJ, Gabrieli JD. Immature frontal lobe contributions to cognitive control in children: Evidence from fMRI. Neuron. 2002; 33:301–311. [PubMed: 11804576]

Cabeza R, Nyberg L. Imaging cognition II: An empirical review of 275 PET and fMRI studies. J Cogn Neurosci. 2000; 12:1–47. [PubMed: 10769304]

Carroll, JB.; Davies, P.; Richman, B. The American Heritage Word Frequency Book. Boston, MA: Houghton Mifflin; 1971.

Dupont S, Van de Moortele PF, Samson S, Hasboun D, Poline JB, Adam C, Lehericy S, Le Bihan D, Samson Y, Baulac M. Episodic memory in left temporal lobe epilepsy: A functional MRI study. Brain. 2000; 123 (Part 8):1722–1732. [PubMed: 10908201]

Fernandez G, de Greiff A, von Oertzen J, Reuber M, Lun S, Klaver P, Ruhlmann J, Reul J, Elger CE. Language mapping in less than 15 minutes: Real-time functional MRI during routine clinical investigation. Neuroimage. 2001; 14:585–594. [PubMed: 11506532]

Forman S, Cohen J, Fitzgerald M, Eddy W, Mintun M, Noll D. Improved assessment of significant activation in functional magnetic resonance imaging (fMRI) Use of a cluster-size threshold. Magn Reson Med. 1995; 33:636–647. [PubMed: 7596267]

Friston K, Worsley K, Frackowiak R, Mazziotta J, Evans A. Assessing the significance of focal activations using their spatial extent. Hum Brain Map. 1994; 1:210–220.

Frost JA, Binder JR, Springer JA, Hammeke TA, Bellgowan PS, Rao SM, Cox RW. Language processing is strongly left lateralized in both sexes. Evidence from functional MRI. Brain. 1999; 122 (Part 2):199–208. [PubMed: 10071049]

Gaillard WD. Functional MR imaging of language, memory, and sensorimotor cortex. Neuroimaging Clin N Am. 2004; 14:471–485. [PubMed: 15324859]

Gaillard WD, Balsamo L, Xu B, Grandin CB, Braniecki SH, Papero PH, Weinstein S, Conry J, Pearl PL, Sachs B, Sato S, Jabbari B, Vezina LG, Frattali C, Theodore WH. Language dominance in partial epilepsy patients identified with an fMRI reading task. Neurology. 2002; 59:256–265. [PubMed: 12136067]

Gaillard WD, Balsamo L, Xu B, McKinney C, Papero PH, Weinstein S, Conry J, Pearl PL, Sachs B, Sato S, Vezina LG, Frattali C, Theodore WH. fMRI language task panel improves determination of language dominance. Neurology. 2004; 63:1403–1408. [PubMed: 15505156]

Gaillard WD, Berl MM, Moore EN, Ritzl EK, Rosenberger LR, Weinstein SL, Conry JA, Pearl PL, Ritter FF, Sato S, Vezina LG, Vaidya CJ, Wiggs E, Fratalli C, Risse G, Ratner NB, Gioia G, Theodore WH. Atypical language in lesional and nonlesional complex partial epilepsy. Neurology. 2007; 69:1761–1771. [PubMed: 17967992]

Hamberger MJ, McClelland S III, McKhann GM II, Williams AC, Goodman RR. Distribution of auditory and visual naming sites in nonlesional temporal lobe epilepsy patients and patients with space-occupying temporal lobe lesions. Epilepsia. 2007; 48:531–538. [PubMed: 17326797]

Hampson M, Peterson B, Skudlarski P, Gatenby J, Gore J. Detection of functional connectivity using temporal correlations in MR images. Hum Brain Mapp. 2002; 15:247–262. [PubMed: 11835612]

Harris, AJ. Harris Tests of Lateral Dominance: Manual of Directions for Administration and Interpretation. New York: David McKay Co., Inc; 1974.

Jenkinson M, Bannister P, Brady M, Smith S. Improved optimization for the robust and accurate linear registration and motion correction of brain images. Neuroimage. 2002; 17:825–841. [PubMed: 12377157]

Jenkinson M, Smith S. A global optimization method for robust affine registration of brain images. Med Image Anal. 2001; 5:143–156. [PubMed: 11516708]

Just MA, Carpenter PA, Keller TA, Eddy WF, Thulborn KR. Brain activation modulated by sentence comprehension. Science. 1996; 274:114–116. [PubMed: 8810246]

Khedr EM, Hamed E, Said A, Basahi J. Handedness and language cerebral lateralization. Eur J Appl Physiol. 2002; 87:469–473. [PubMed: 12172889]

Knecht S, Drager B, Deppe M, Bobe L, Lohmann H, Floel A, Ringelstein EB, Henningsen H. Handedness and hemispheric language dominance in healthy humans. Brain. 2000; 123 (Part 12): 2512–2518. [PubMed: 11099452]

Kurthen M, Helmstaedter C, Linke DB, Hufnagel A, Elger CE, Schramm J. Quantitative and qualitative evaluation of patterns of cerebral language dominance. An amobarbital study. Brain Lang. 1994; 46:536–564. [PubMed: 8044676]

Lahlou, M.; Guillen, MR.; Adjouadi, M.; Gaillard, WD. An Online Web-Based Repository Site of fMRI Medical Images and Clinical Data for Childhood Epilepsy. Ontario, Canada. The 11th World Congress on Internet in Medicine; Mednet; 2006. p. 120-127.

Liegeois F, Connelly A, Cross JH, Boyd SG, Gadian DG, Vargha-Khadem F, Baldeweg T. Language reorganization in children with early-onset lesions of the left hemisphere: An fMRI study. Brain. 2004; 127 (Part 6):1229–1236. [PubMed: 15069021]

Mbwana J, Berl MM, Ritzl EK, Rosenberger L, Mayo J, Weinstein S, Conry JA, Pearl PL, Shamim S, Moore EN, Sato S, Vezina LG, Theodore WH, Gaillard WD. Limitations to plasticity of language network reorganization in localization related epilepsy. Brain. 2009; 132 (Part 2):347–356. [PubMed: 19059978]

Muller R, Rothermel R, Behen M, Muzik O, Mangner T, Chugani H. Developmental changes of cortical and cerebellar motor control: A clinical positron emission tomography study with children and adults. J Child Neurol. 1998a; 13:550. [PubMed: 9853648]

Muller R, Rothermel R, Muzik O, Becker C, Fuerst D, Behen M, Mangner T, Chugani H. Determination of language dominance by [15O]-water PET in children and adolescents: A comparison with the Wada test. J Epilepsy. 1998b; 11:152–161.

Ojemann G, Ojemann J, Lettich E, Berger M. Cortical language localization in left, dominant hemisphere. An electrical stimulation mapping investigation in 117 patients. J Neurosurg. 2008; 108:411–421. [PubMed: 18240946]

Oldfield R. The assessment and analysis of handedness: The Edinburgh inventory. Neuropsychologia. 1971; 9:97–113. [PubMed: 5146491]

Petersen SE, Fox PT, Posner MI, Mintun M, Raichle ME. Positron emission tomographic studies of the cortical anatomy of single-word processing. Nature. 1988; 331:585–589. [PubMed: 3277066]

Price CJ, Crinion J, Friston KJ. Design and analysis of fMRI studies with neurologically impaired patients. J Magn Reson Imaging. 2006; 23:816–826. [PubMed: 16649208]

Pujol J, Deus J, Losilla JM, Capdevila A. Cerebral lateralization of language in normal left-handed people studied by functional MRI. Neurology. 1999; 52:1038–1043. [PubMed: 10102425]

Ramsey NF, Sommer IE, Rutten GJ, Kahn RS. Combined analysis of language tasks in fMRI improves assessment of hemispheric dominance for language functions in individual subjects. Neuroimage. 2001; 13:719–733. [PubMed: 11305899]

Rasmussen T, Milner B. The role of early left-brain injury in determining lateralization of cerebral speech functions. Ann N Y Acad Sci. 1977; 299:355–369. [PubMed: 101116]

Risse GL, Gates JR, Fangman MC. A reconsideration of bilateral language representation based on the intracarotid amobarbital procedure. Brain Cogn. 1997; 33:118–132. [PubMed: 9056279]

Rosenberger LR, Zeck J, Berl MM, Moore EN, Ritzl EK, Shamim S, Weinstein SL, Conry JA, Pearl PL, Sato S, Vezina LG, Theodore WH, Gaillard WD. Interhemispheric and intrahemispheric language reorganization in complex partial epilepsy. Neurology. 2009; 72:1830–1836. [PubMed: 19470965]

Rowe DB, Hoffmann RG. Multivariate statistical analysis in fMRI. IEEE Eng Med Biol Mag. 2006; 25:60–64. [PubMed: 16568938]

Seghier M, Lazeyras F, Pegna A, Annoni J, Khateb A. Group analysis and the subject factor in functional magnetic resonance imaging: Analysis of fifty right-handed healthy subjects in a semantic language task. Hum Brain Mapp. 2008:29.

Smith SM. Fast robust automated brain extraction. Hum Brain Mapp. 2002; 17:143–155. [PubMed: 12391568]

Spreer J, Arnold S, Quiske A, Wohlfarth R, Ziyeh S, Altenmuller D, Herpers M, Kassubek J, Klisch J, Steinhoff BJ, Honegger J, Schulze-Bonhage A, Schumacher M. Determination of hemisphere dominance for language: Comparison of frontal and temporal fMRI activation with intracarotid amytal testing. Neuroradiology. 2002; 44:467–474. [PubMed: 12070719]

Springer JA, Binder JR, Hammeke TA, Swanson SJ, Frost JA, Bellgowan PS, Brewer CC, Perry HM, Morris GL, Mueller WM. Language dominance in neurologically normal and epilepsy subjects: A functional MRI study. Brain. 1999; 122 (Part 11):2033–2046. [PubMed: 10545389]

Staudt M, Grodd W, Niemann G, Wildgruber D, Erb M, Krageloh-Mann I. Early left periventricular brain lesions induce right hemispheric organization of speech. Neurology. 2001; 57:122–125. [PubMed: 11445639]

Staudt M, Lidzba K, Grodd W, Wildgruber D, Erb M, Krageloh-Mann I. Right-hemispheric organization of language following early left-sided brain lesions: Functional MRI topography. Neuroimage. 2002; 16:954–967. [PubMed: 12202083]

Stoodley CJ, Schmahmann JD. Functional topography in the human cerebellum: A meta-analysis of neuroimaging studies. Neuroimage. 2009; 44:489–501. [PubMed: 18835452]

Sugiura M, Watanabe J, Maeda Y, Matsue Y, Fukuda H, Kawashima R. Different roles of the frontal and parietal regions in memory-guided saccade: A PCA approach on time course of BOLD signal changes. Hum Brain Mapp. 2004; 23:129–139. [PubMed: 15449357]

Sui J, Adali T, Pearlson GD, Calhoun VD. An ICA-based method for the identification of optimal FMRI features and components using combined group-discriminative techniques. Neuroimage. 2009; 46:73–86. [PubMed: 19457398]

Szaflarski JP, Binder JR, Possing ET, McKiernan KA, Ward BD, Hammeke TA. Language lateralization in left-handed and ambidextrous people: fMRI data. Neurology. 2002; 59:238–244. [PubMed: 12136064]

Szaflarski JP, Schmithorst VJ, Altaye M, Byars AW, Ret J, Plante E, Holland SK. A longitudinal functional magnetic resonance imaging study of language development in children 5 to 11 years old. Ann Neurol. 2006; 59:796–807. [PubMed: 16498622]

Turkeltaub PE, Gareau L, Flowers DL, Zeffiro TA, Eden GF. Development of neural mechanisms for reading. Nat Neurosci. 2003; 6:767–773. [PubMed: 12754516]

Turkeltaub PE, Flowers DL, Verbalis A, Miranda M, Gareau L, Eden GF. The neural basis of hyperlexic reading: An FMRI case study. Neuron. 2004; 41:11–25. [PubMed: 14715131]

Vaidya C, Bunge S, Dudukovic N, Zalecki C, Elliott G, Gabrieli J. Altered neural substrates of cognitive control in childhood ADHD: Evidence from functional magnetic resonance imaging. Am J Psychiatry. 2005; 162:1605. [PubMed: 16135618]

Viviani R, Gron G, Spitzer M. Functional principal component analysis of fMRI data. Hum Brain Mapp. 2005; 24:109–129. [PubMed: 15468155]

Voets NL, Adcock JE, Flitney DE, Behrens TE, Hart Y, Stacey R, Carpenter K, Matthews PM. Distinct right frontal lobe activation in language processing following left hemisphere injury. Brain. 2006; 129 (Part 3):754–766. [PubMed: 16280351]

Weber B, Wellmer J, Reuber M, Mormann F, Weis S, Urbach H, Ruhlmann J, Elger C, Fernandez G. Left hippocampal pathology is associated with atypical language lateralization in patients with focal epilepsy. Brain. 2006; 129:346. [PubMed: 16330504]

Wise R, Chollet F, Hadar U, Friston K, Hoffner E, Frackowiak R. Distribution of cortical neural networks involved in word comprehension and word retrieval. Brain. 1991; 114 (Part 4):1803–1817. [PubMed: 1884179]

Woermann FG, Jokeit H, Luerding R, Freitag H, Schulz R, Guertler S, Okujava M, Wolf P, Tuxhorn I, Ebner A. Language lateralization by Wada test and fMRI in 100 patients with epilepsy. Neurology. 2003; 61:699–701. [PubMed: 12963768]

Woods RP, Dodrill CB, Ojemann GA. Brain injury, handedness, and speech lateralization in a series of amobarbital studies. Ann Neurol. 1988; 23:510–518. [PubMed: 3389757]

Woolrich MW, Ripley BD, Brady M, Smith SM. Temporal autocorrelation in univariate linear modeling of FMRI data. Neuroimage. 2001; 14:1370–1386. [PubMed: 11707093]

Worsley K, Evans A, Marrett S, Neelin P. A three-dimensional statistical analysis for CBF activation studies in human brain. J Cerebr Blood Flow Metab. 1992; 12:900–900.

Wyllie E, Naugle R, Chelune G, Luders H, Morris H, Skibinski C. Intracarotid amobarbital procedure: II. Lateralizing value in evaluation for temporal lobectomy. Epilepsia. 1991; 32:865–869. [PubMed: 1743158]

You X, Guillen M, Bernal B, Gaillard WD, Adjouadi M. fMRI activation pattern recognition: A novel application of PCA in language network of pediatric localization related epilepsy. Conf Proc IEEE Eng Med Biol Soc. 2009; 1:5397–5400. [PubMed: 19963905]

APPENDIX A: PCA-DISTANCE METHOD ON ACTIVATION MAPS

PCA-distance method on activation maps were generated according to the following steps:

1. Each individual's 3D dataset was transformed into a 1D dataset with n voxels, where n is defined by $M \times N \times L$, where M, N, and L are the dimensions of the activation map image in the x, y, and z axes. The whole population of k subjects was organized on a 2D matrix X, where each subject constitutes a specific column x_i in the matrix. The mean value for each voxel across all subjects, and the mean vector m of these k subjects were computed.

2. The covariance matrix Cx of X was calculated from Eq. (1). Each activation map was centered by subtracting the mean as indicated in Eq. (3).

$$Cx = \Psi^T \Psi \quad (1)$$

where

$$\Psi = [\Phi_1 \Phi_2 \ldots \Phi_k] \quad (2)$$

$$\Phi_i = x_i - m \quad i = 1, 2, \ldots, k \quad (3)$$

3. Once the eigenvectors of the covariance matrix (Cx) were calculated, then eigenvectors were sorted by the corresponding eigenvalues to generate the matrix E as in Eq. (4). Each subject was represented by a row vector $e_{.i} = [e_{1i}.e_{ji}]$ where j corresponded to the number of eigenvectors being used.

$$E=[\ e_1\quad e_2\ldots e_k\ ]=\begin{bmatrix} e_{11} & e_{21} & \ldots & \ldots & e_{k1} \\ e_{12} & e_{22} & \ldots & \ldots & e_{k2} \\ .. & \ldots & \ldots & \ldots & .. \\ .. & \ldots & \ldots & \ldots & .. \\ e_{1k} & \ldots & \ldots & \ldots & e_{kk} \end{bmatrix} \quad (4)$$

$$U=\Psi E \quad (5)$$

Notice that the E matrix is equivalent to the subject loading matrix as in SSM and the U matrix calculated in Eq. (5) is equivalent to the regional covariance pattern, but instead of "regional," our U is the covariance patterns of the whole 3D brain region.

Figure A1 is about the first two subjects loading coefficients, which are equal to the first two eigenvectors.

4. On the basis of the e_i distribution in the E matrix and the observation of the relationship of the top two eigenvectors (as shown in the Appendix B), three primary clusters with far distances from each other were first determined. Then, the new mean (m_{new}) vector of these clusters was generated with subjects only chosen from the three primary clusters, and the principal components of these clusters were calculated, generating the new U_{new} matrix following Eq. (5).

5. To group subjects' activation maps not falling in any of the primary clusters (undecided regions), vector x_{new} will now represent the activation map of the subject, and the distance method is used to determine to which cluster it is closest. The following steps are undertaken:

I. Project Φ_{new}, which is the new centered x_{new} ($\Phi_{\text{new}} = x_{\text{new}} - m_{\text{new}}$), onto the primary clusters defined eigenspace using Eq. (6).

$$\widehat{\Phi}_{\text{new}}=\sum_{l=1}^{j} u_l^T \Phi_{\text{new}} u_l \quad (6)$$

where each u_l represents a column vector of the U_{new} matrix as described in step (4).

II. Calculate the Euclidean distance feature using Eq. (7) below:

$$D_i=|\widehat{\Phi}_{\text{new}}-\Phi_i| \quad (7)$$

for i 1,2,…,q, where q is the number of primary cluster members, with Φ_i $x_i - m_{\text{new}}$ and where j($j < k$) is the number of eigenvectors selected. (In the study, j was tried from 3 to 7, and the separation results were found the same, which shows that the top eigenvectors already includes enough info of the population.)

III. The new subject was assigned to the cluster whose member Φ_i had the minimum distance calculated through Eq. (7). In other words, the new subject is assigned to the cluster where the closest identified subject Φ_i was located.

Figure A2 is the clustering results showing in the top three subject loadings using the top two eigenvectors' feature as criteria to select primary clusters, and the projection distance onto the top three eigenfaces out of the primary clusters' decisional space. (Separation results of 3–7 eigenfaces were found the same).

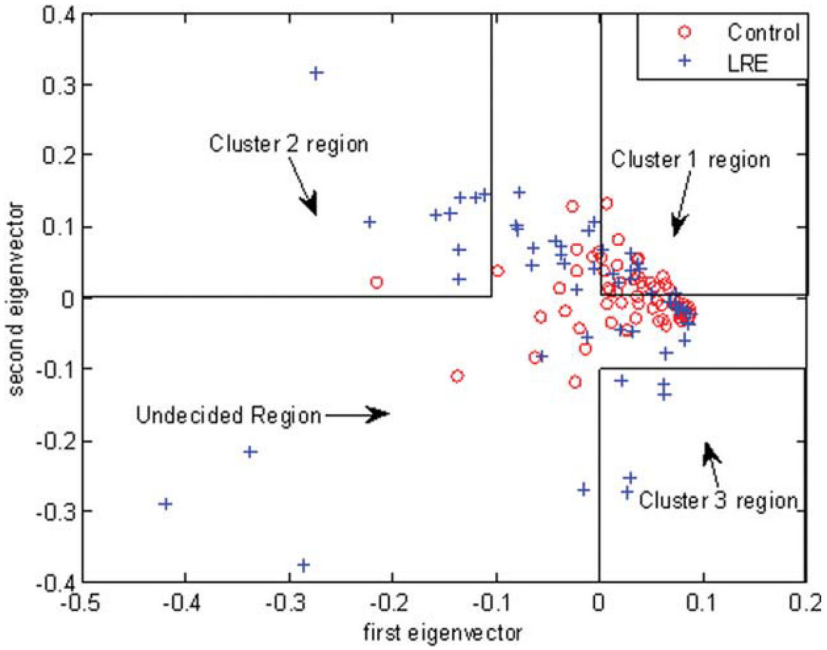

Figure A1.

Determination of the primary clusters using the two dominant eigenvectors (with the two highest eigenvalues) of the PCA. These two dominant eigenvectors are used to select three primary clusters based on the following decision rules: Group 1: $e_{1i} < 0 \cap e_{2i} > 0$ (which is the most condensed cluster region with 32 data points); Group 2: $e_{1i} < -0.1 \cap e_{2i} > 0$ (with 10 data points); Group 3: $e_{1i} > 0 \cap e_{2i} < -0.1$ (with five data points). The undecided region, with 75 data points, is the remaining region outside these three clusters. [Color figure can be viewed in the online issue, which is available at wileyonlinelibrary.com.]

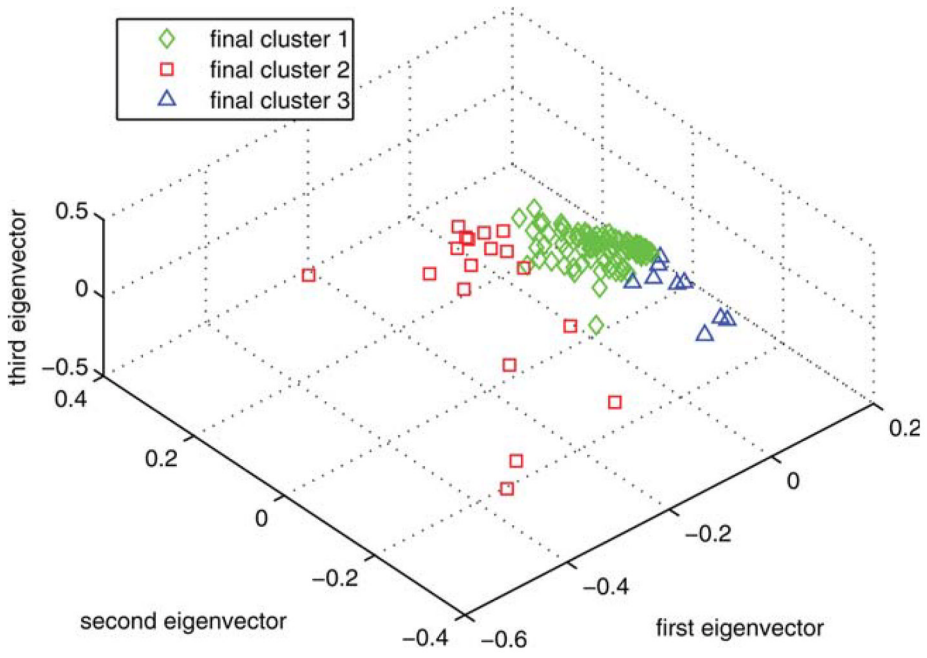

Figure A2.
Final clusters distribution in the top three eigenvectors' space. [Color figure can be viewed in the online issue, which is available at wileyonlinelibrary.com.]

APPENDIX B: PROCESS OF DECIDING THE PRIMARY CLUSTER CHOSEN CRITERIA

The process of choosing the top two eigenvectors is based on the cumulated eigenvalues of the PCA as shown in Figure B1. In terms of the clusters, the initial clustering stage helped us to cluster 47 out of 122 (39%) of the population. It is worthy to mention, that this first round of clustering was achieved based on the information provided by the first two eigenvectors of the system. In other words, the first two eigenvectors carry significant feature information about intensity differences and overall lateralization of the activation (note that the sum of the first two most significant eigenvalues is around 80% of the total sum as seen in Figure B1, which means that the mean square error is 20%). See Figure B1 below.

As a consequence, the information provided by the first two eigenvectors was not sufficient to define absolute boundaries for clustering all the subjects into their respective groups. Because of that, we decided to identify primary clusters, leaving the subjects as indeterminate in the overlapping area defined by the plane e_1–e_2. Figure A1 depicts the criteria used to select the members of the three primary clusters.

These clustering rules were based on our findings on the results shown in Figures B2–B7. Please note that in these figures the selection of the symbols used to denote the different groups is made for appropriate visualization of the different clusters of data and also to avoid any ambiguity associated when such symbols overlap with each other.

It was determined that when considering any two groups in the population, either higher intensity typical versus atypical, or lower intensity typical versus atypical, or even higher intensity typical versus lower intensity typical, the zero line of the first eigenvector is sufficient to separate them as given in Figures B2 through B4. Higher activation intensity

was defined as higher than the mid point of the intensity range of the analyzed population's means. On the other hand, lower activation intensity was defined as lower than the mean of the analyzed population's intensity. Within these two points (the mean of the population and the mid point of the means) was a range we determined as normal intensities.

With all the 122 subjects considered, it was determined that the second eigenvector as the *x* axis tends to separate typical from atypical when the overall LI is used as the *y* axis (as in Fig. B5), whereas the first eigenvector tends to separate higher intensity from lower intensity (as in Fig. B6).

After applying the distance method on the undecided subjects, the final clustering results are as shown in Figure A2. We also used a dendrogram to affirm that there are indeed mainly three groups in the population as seen from Figure B7.

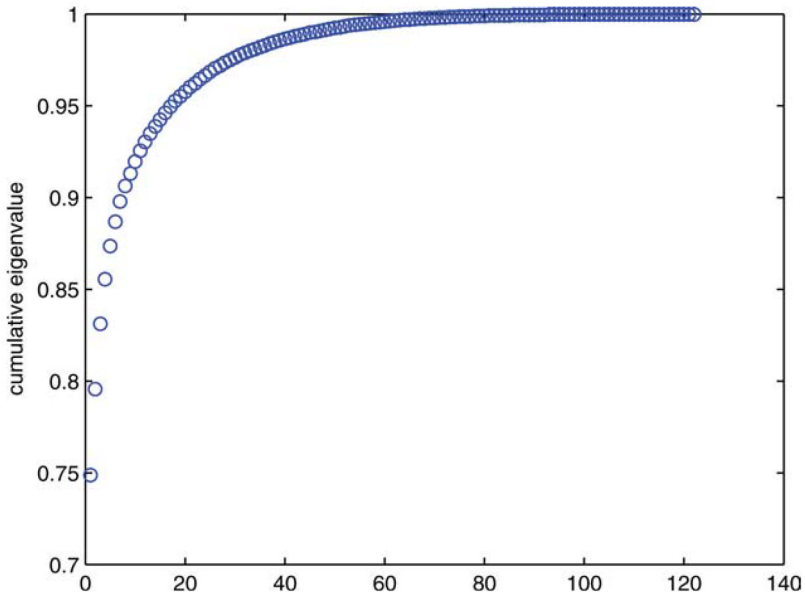

Figure B1.
Cumulative eigenvalues for the 122 subjects. Note the top two eigenvectors provide 80% of the eigenvalues. [Color figure can be viewed in the online issue, which is available at wileyonlinelibrary. com.]

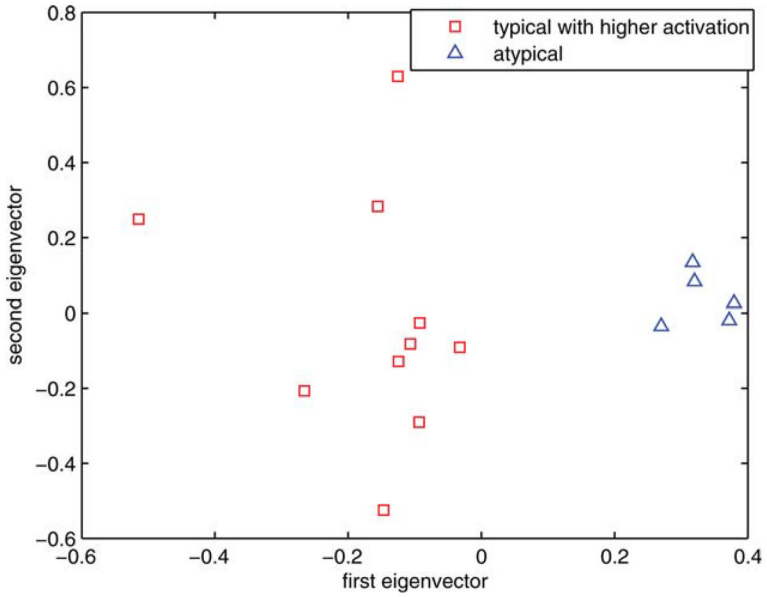

Figure B2.
The zero line in the first eigenvector axis is determined to provide a consistent decision line between higher intensity typical group (<0) and atypical group (>0). [Color figure can be viewed in the online issue, which is available at wileyonlinelibrary.com.]

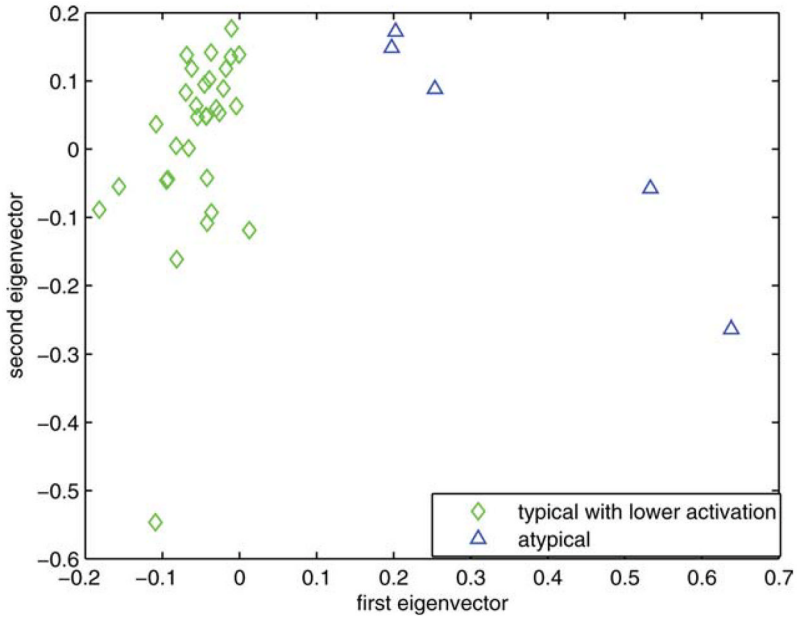

Figure B3.
The zero line in the first eigenvector axis is determined to provide a consistent decision line between lower intensity typical group (<0) and atypical group (>0). [Color figure can be viewed in the online issue, which is available at wileyonlinelibrary.com.]

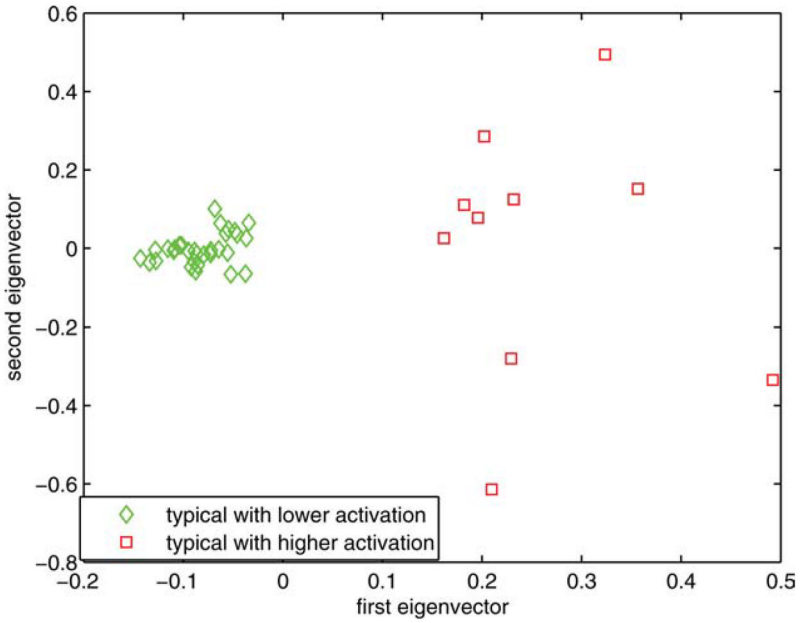

Figure B4.
The zero line in the first eigenvector axis is determined to provide a consistent decision line between higher intensity group (>0) and lower intensity groups (<0) within all the subjects that are typical. [Color figure can be viewed in the online issue, which is available at wileyonlinelibrary.com.]

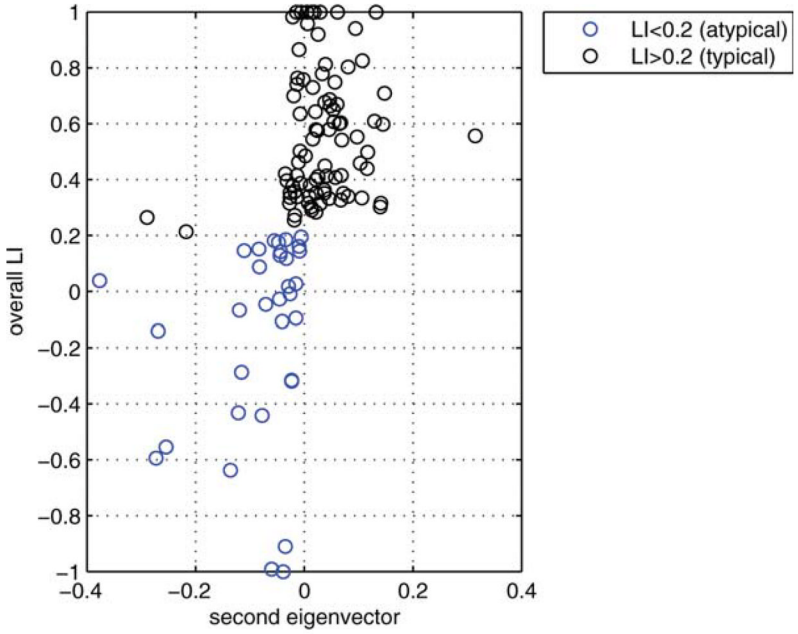

Figure B5.
The zero line in the second eigenvector axis provides intuitively a rough decision line between typical (>0) and atypical groups (<0). Note that every data point that is on the right side of this decision line are actually left dominant (LI > 0.2). In this figure, since the mean of the second eigenvector values for those globally atypical (LI < 0.2) is −0.0814, and since the mean of the second eigenvector values for those globally right dominant (LI < −0.2) is

−0.1051, the −0.1 value (an approximate in-between these two means) was chosen as a threshold criteria for primary cluster 3 as can be seen in Figure A1. Combined with the results given in Figure B2 through Figure B4, $e_1 > 0$ and $e_2 < -0.1$ were thus chosen as the boundaries for primary cluster 3 (atypical group). [Color figure can be viewed in the online issue, which is available at wileyonlinelibrary.com.]

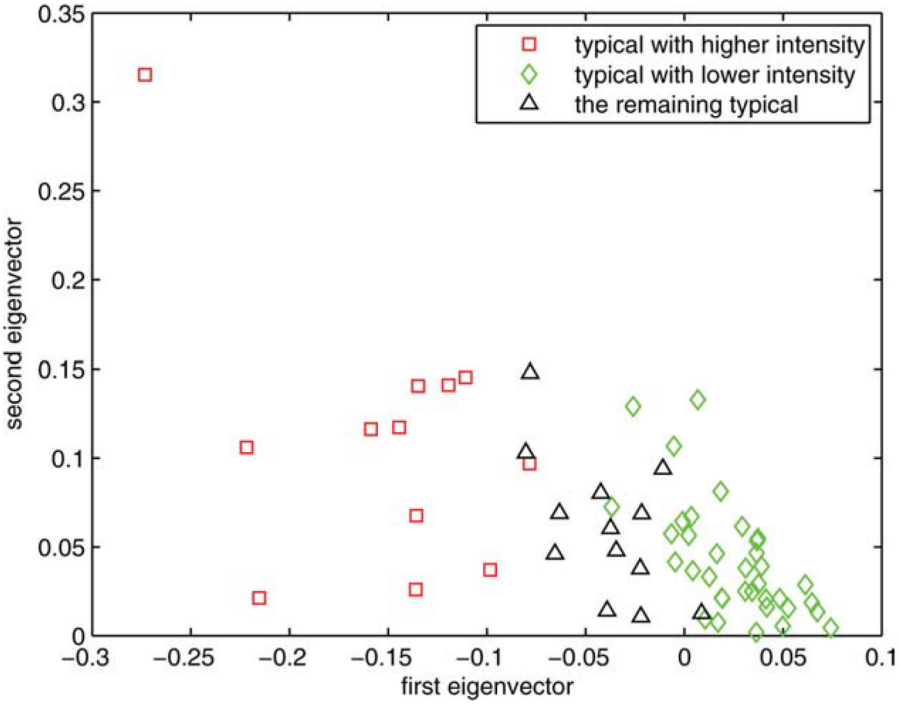

Figure B6.

On the basis of the results shown in Figure B5, and considering only the typical subjects that satisfied the condition $e_2 > 0$, this plot reflects the subjects' distribution based on intensity. The red squares are those subjects whose intensities are higher than the mid point of the intensity range of the analyzed population's means; green diamonds are the ones that are lower than the mean activation intensity of these typical subjects. That is why the −0.1 value for e_1 was chosen as the primary cluster threshold for the higher intensity group and 0 for lower intensity group. Combined with the results given in Figure B2 through Figure B5, $e_1 < -0.1$ and $e_2 > 0$ were chosen as the boundary for primary cluster 2 (the higher intensity typical group), $e_1 > 0$ and $e_2 > 0$ were chosen as the boundary for primary cluster 1 (the lower intensity typical group). [Color figure can be viewed in the online issue, which is available at wileyonlinelibrary.com.]

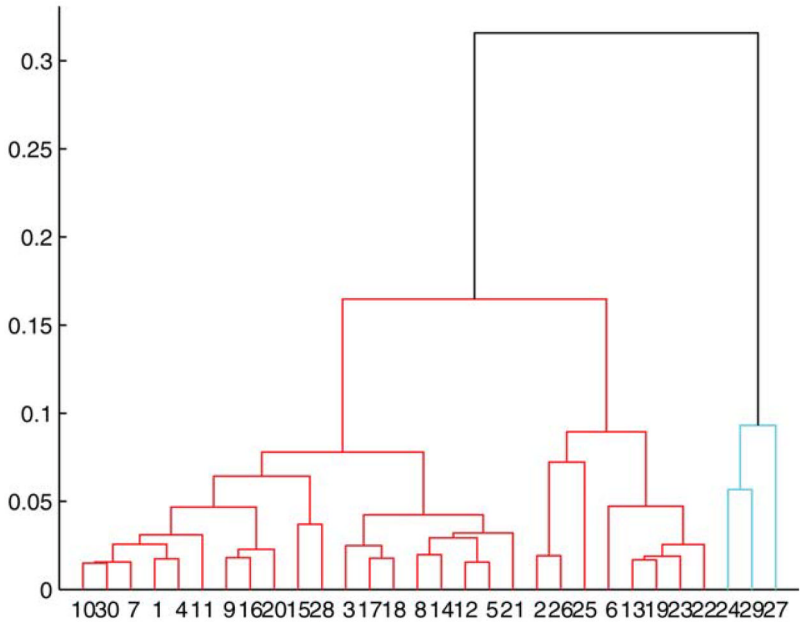

Figure B7.
The dendrogram of the Euclidian distance matrix of the PCA suggesting there are at least three subgroups within the subjects. [Color figure can be viewed in the online issue, which is available at wileyonlinelibrary.com.]

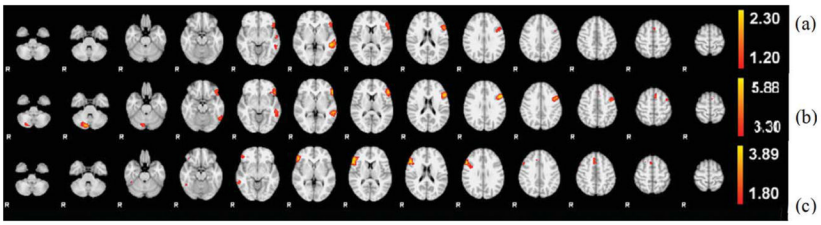

Figure 1.

2D array of selected axial cuts for color-coded activation intensities depicting the axial view of the mean activation maps for each group. Higher activations are in yellow color. Brain is oriented in radiological convention: right hemisphere on the left side. (**a**) Mean activation map for Group 1 with strong left lateralization of anterior (Broca) and posterior (Wernicke) clusters. (**b**) Mean activation map for Group 2 with higher mean intensity range than (a), which explains the better definition of supplementary motor area (SMA). (**c**) Mean activation map for Group 3 with an atypical right hemisphere dominant response, particularly, the anterior (Broca) cluster. Different intensity threshold (90% of the energy) was used for visualization purpose.

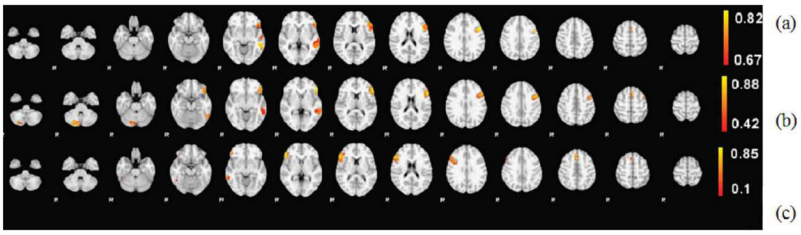

Figure 2.
Commonality significance maps of each group. All three groups have the highest significance value higher than 0.8 and Group 1 (**a**) has the least variance among the group members in the activated area, whereas Group 3 (**c**) has the largest variance.

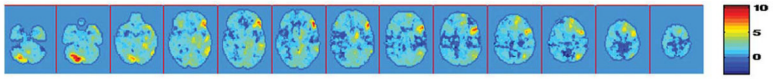

Figure 3.
Second level *t*-test for comparing the mean maps between Groups 1 and 2. Note the high *t* values (significant level $P < 0.01$) in the shared activated area, which is in the left IFG and MFG.

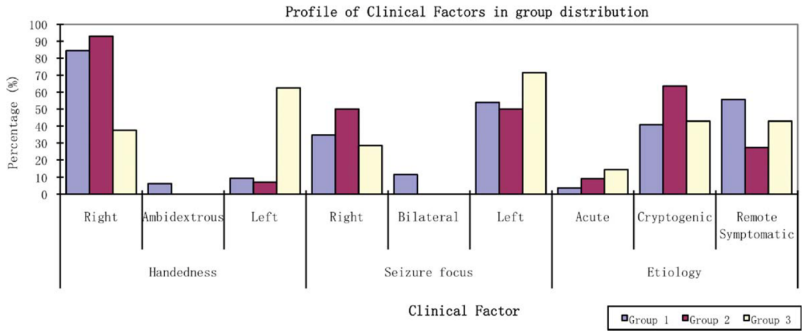

Figure 4.

Clinical factors distribution among three groups. The percentage of patients in each group based on handedness, seizure focus, and seizure etiology findings. Handedness was different among the three groups, and between Group 1 versus Group 3, and between Group (1 + 2) versus Group 3. ($P < 0.0167$ Holm's sequential Bonferroni correction).

TABLE I

Subjects distribution by institution and scanner type*

Subjects		Institution	Scanner	TR	Voxel size (mm)	Num
LRE	HSC	Hospital for Sick Children (Toronto, Canada)	GE 1.5 T	2	3.44 × 3.44 × 5	19
	MCH	Miami Children's Hospital (Miami, FL)	Phillips Intera 1.5 T	2	3.75 × 3.75 × 8	10
	CNMC	Children's National Medical Center (Washington, DC)	Siemens Trio 3 T	2	3.44 × 3.44 × 4	14
	BCCH	BC Children's Hospital (Vancouver, Canada)	Siemens Avanto 1.5 T	3	3.44 × 3.44 × 3.5	4
	CHOP	Children's Hospital of Philadelphia (PA)	Siemens Trio 3 T	3	3.0 × 3.0 × 3.0	11
Control	CNMC	Children's National Medical Center (Washington, DC)	Siemens Trio 3 T	3	3.0 × 3.0 × 3.0	64

*No-activation cases were not taken into account.

TABLE II

Distribution of basic demographic data

	Patients	Controls
Number	58	64
Male (%)	63.79	54.69
Atypical handedness (%)	19	0
Mean age (years)	13.86 (4.5–19)	8.65 (4.2–12.9)
Mean age of seizure onset	8.23 (1–18)	—
Temporal focus of left localized (%)	65	—
Temporal focus of right localized (%)	39	—
Mean duration of seizures (min)	2.88	—

TABLE III

Activation location, size, peak values, and commonality significance value for each group map*

Group	Cluster size	Mean-*Z* (peak)	C_s of the peak	*x*, *y*, *z* (Voxel space+)	Region (BA)
1	319	1.91	0.74	48, 47, 31	LIFG (44)
	248	2.3	0.74	48, 29, 24	LMTG (21)
	10	1.42	0.76	32, 47, 41	RIFG (32)
2	1014	5.88	0.80	48, 47, 32	LIFG (44/45)
	416	5.2	0.68	49, 29, 23	LMTG (21)
	338	5.24	0.73	26, 15, 12	R cerebellum
	147	4.26	0.72	32, 46, 42	RMFG (46)
3	500	3.89	0.66	12, 50, 28	RIFG (45/48)
	61	2.51	0.71	29, 52, 40	RMTG (8)
	35	2.78	0.46	11, 27, 22	RMFG (37/20)

*The cluster size here reflects the number of thresholded voxels within the cluster of the mean activation map. Threshold values are 1.2 for group Group 1, 3.3 for group Group 2, 1.8 for Group 3, same as the threshold used for visualization purpose in Figure 1, containing 90% of the activation energy. The largest cluster in Group 2 has a maxima in IFG but extends into left MFG.

+The Voxel Space we use here is the FSL MNI space, using coordinates as: *x*-axis as the right–left direction (moving in the left direction increases the *x* voxel index, range: 1–61); *y*-axis as the posterior–anterior direction (moving in the anterior direction increases the *y* voxel index, range: 1–73); *z*-axis as the inferior–superior direction (moving in the superior direction increases the *z* voxel index, range: 1–61).

TABLE IV

Profile of clinical factors of three groups divided by PCA method

Clinical factors		PCA groups 1	2	3
Handedness *	Ambidextrous	2	0	0
	Right	27	13	3
	Left	3	1	5
	N/A	3	1	0
	Total	35	15	8
Seizure focus	Bilateral	3	0	0
	Right	9	7	2
	Left	14	7	5
	N/A	9	1	1
	Total	35	15	8
Etiology	Acute	1	1	1
	Cryptogenic	11	7	3
	Remote symptomatic	15	3	3
	N/A	8	4	1
	Total	35	15	8
Gender	Male	23	8	6
	Female	12	7	2
	Total	35	15	8

* Fisher exact test, comparison among Groups 1–3, $P = 0.007$ ($P < 0.0167$ Holm's sequential Bonferroni correction). Holm's sequential Bonferroni correction procedure: Since the overall difference among the three groups is significant in handedness (Fisher exact test, $P = 0.0079$), now comparing the smallest P value first, which is between Groups 1 and 3 $P = 0.007 < 0.05/3, 0.0167$, so it's significant; now compare the second smallest one between Groups 2 and 3, $P = 0.02 < 0.05/2, 0.025$, still significant; but the third significant P value between Groups 1 and 2, 0.6 is not significant.

TABLE V

Distribution of handedness across three groups with regard to seizure focus *

		Seizure focus								
		Left			Right			Bilateral		
Handedness		**1**	**2**	**3**	**1**	**2**	**3**	**1**	**2**	**3**
Left	1	1			2			0		
	2		0			1			0	
	3			3			1			0
Right	1	12			7			3		
	2		7			6			0	
	3			2			1			0
Ambidextrous	1	1			0			0		
	2		0			0			0	
	3			0			0			0

* Only 47 datasets combined the information on seizure focus and handedness. Notice the numbers are too few in some subgroups to make statistical comparisons meaningful.